(CCl_4) model] and subsequent proliferation and have reported that in the specific environment of chronic inflammation, bone marrow cells differentiate to albumin-positive cells with a certain efficiency. In that process, liver functions, liver fibrosis, and survival rate all show significant improvements (4 – 6). Therefore, a clinical study [Autologous Bone Marrow Cell Infusion (ABM*i*) Therapy] was started in November 2003 based on the results of these basic studies (7). In addition, in 2005, a multicenter clinical trial, a liver regeneration with cell transplantation (LRCT) study, was started. As of the time of this writing, other clinical trials for a liver regeneration are also being conducted in Korea, India, Brazil, Germany, and Iran (3). During this same period, new cell therapies have been developed, including cell therapy using CD34-positive cells induced with granulocyte-colony stimulating factor (G-CSF) in the UK (8, 9) and a therapy with portal administration of CD133-positive mononuclear cells in Germany (10, 11). This article provides an overview of the development of ABM*i* therapy for liver cirrhosis to date, and the future outlook.

2. Basic study: in vivo mouse model of monitoring of bone marrow cells to liver cells and subsequent proliferation (the GFP/CCl_4 model)

We have conducted basic studies using a model of persistent liver damage induced by CCl_4. The GFP/CCl_4 model that we developed and reported has the following characteristics (4, 5) (Fig. 1): 1) an environment of chronic liver damage induced by repeated administration of CCl_4 (2 times/week); 2) the inflammatory condition is also maintained by repeated administration of CCl_4 after bone marrow cell transinfusion; and 3) assuming transinfused autologous bone marrow cells, the donor is a GPP-transgenic mouse that is isogenic with the recipient.

In this model, repeated peritoneal administration of CCl_4 (0.5 ml/kg body) was performed over 4 weeks (8 times) in 6-week-old female C57BL/6 mice to prepare the chronic liver injury and fibrosis (liver cirrhosis) model in mice used as recipients. Cells in whole bone marrow isolated from the femurs of isogenic male GFP transgenic mice were then washed and injected into the recipient mice via a tail vein (peripheral vein). Administration of CCl_4 was continued after this, and the effect in improving liver function was evaluated over time. Improvement in serum albumin levels (4), a significant increase in survival rate, and decreased hepatic fibrosis assessed by Sirius-red staining were seen following administration of bone marrow cells (6). Bone marrow-derived GFP-positive cells were confirmed to produce collegenases, including matrix metalloproteinase (MMP)-2 and -9, during these processes (6). Based on the above basic study, administration of autologous bone marrow cells via a peripheral vein in a chronic liver injury environment is thought to improve liver functions and reduce liver fibrosis and to significantly improve

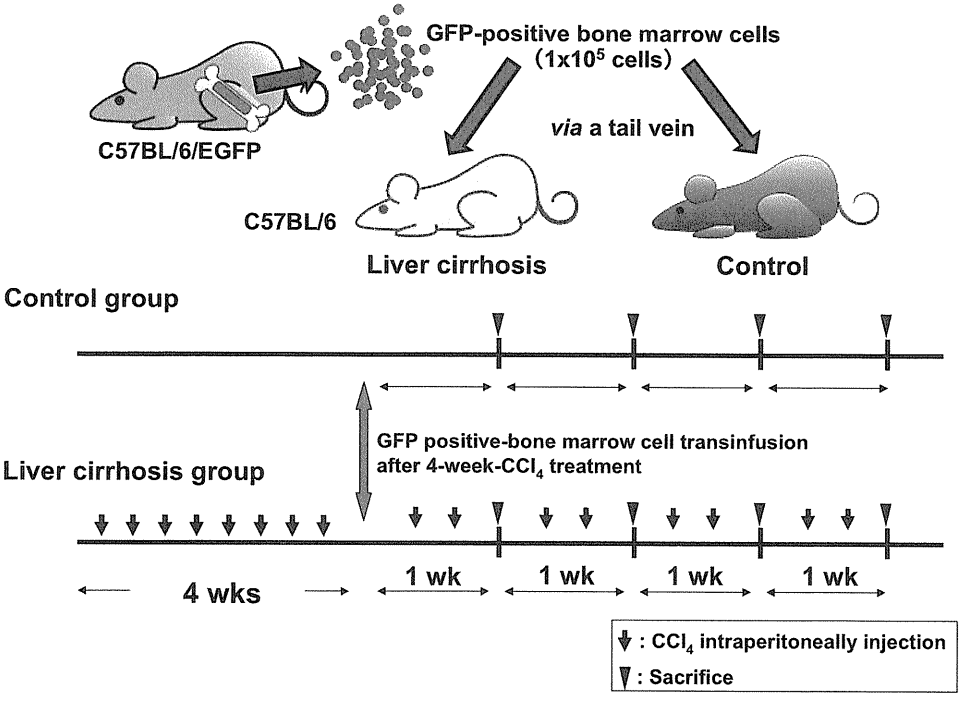

Fig. 1. The mouse GFP/CCl_4 model. The 6-week-old female C57BL/6 mice were treated with CCl_4 twice a week for 4 weeks to induce persistent liver damage. Then 1×10^5 bone marrow mononuclear cells form GFP transgenic C57BL/6 male mice were transinfused through a tail vein. After this transinfusion, CCl_4 treatment twice a week was continued.

vital prognosis in recipients. A later investigation showed that fibroblast growth factor (FGF) has an important function as a factor contributing to this process (12). During early stages of autologous bone marrow cell transinfusion, homeobox-containing genes and helix-loop-helix (HLH) transcriptional regulatory genes were also confirmed to be induced by self-organizing-map-based gene expression (13), and apolipoprotein A1 (apoA1) was induced in serum by proteomics analysis (14), suggesting useful bio-markers for liver regeneration.

3. Clinical study: "Autologous Bone Marrow Cell Infusion Therapy (ABM*i* Therapy) for Decompensated Liver Cirrhosis Patients"

A clinical study called "Autologous Bone Marrow Cell Infusion (ABM*i*) Therapy for Decompensated Liver Cirrhosis Patients" was started in November 2003, building on basic studies with the mouse GFP/CCl_4 model. Details of this clinical study, including indications, are shown as follows:

Treatment indications:

1) Total bilirubin: ≤ 3.0 mg/dl

2) Platelet count: $\geq 5.0 \times 10^{10}$/l

3) Good control of esophagogastric varices and hepatocellular carcinoma

4) Good cardiopulmonary function, and no serious comorbidities

5) No presence of viable hepatocellular carcinoma on computed tomography (CT), magnetic resonance imaging (MRI), or other diagnostic imaging modalities

Protocol:

Autologous bone marrow cells (400 ml) were collected under general anesthesia, and the collected bone marrow fluid was concentrated and washed. Bone marrow mono-

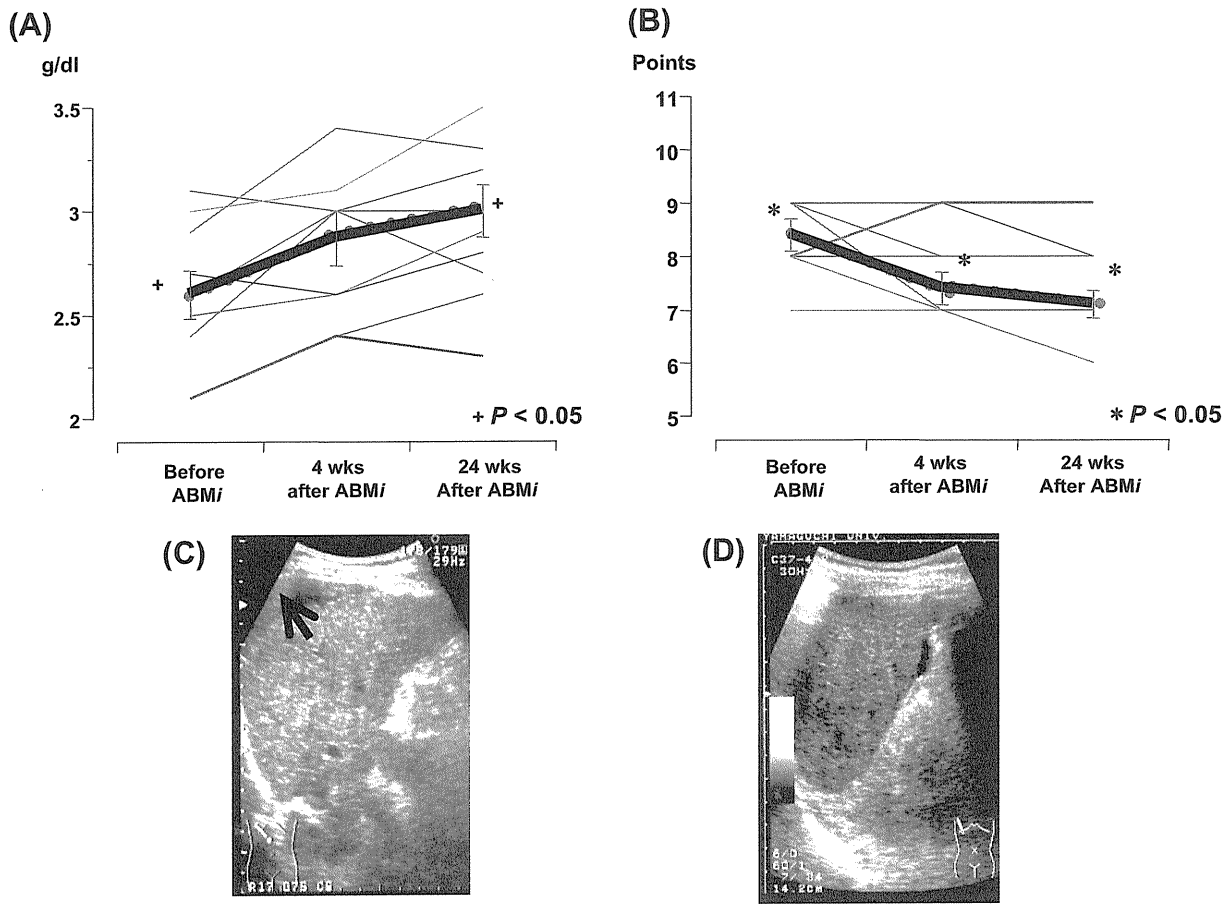

Fig. 2. Liver function improvements in liver cirrhosis patients after autologous bone marrow cell infusion (ABM*i*). A: Serum albumin level (g/dl). The thick line represents the mean value. B: Child-Pugh score (points). The thick line represents the mean value. C and D: Abdominal ultrasound images before and after ABM*i* therapy, respectively. Before ABM*i* therapy, ascites (arrow) is seen on the liver surface (C), but after ABM*i* therapy, clear reductions in ascites are apparent (D). These figures are modified from Ref. 7 with permission.

nuclear cells in that fluid were then purified and condensed according to standard operating procedures (SOP) at the regenerative and cell therapy center, which is fully equipped with good manufacturing practice (GMP) grade facilities, and administered by drip infusion via a peripheral vein to the same patient. The course was observed for 6 months after ABM*i*, and the efficacy and safety were evaluated by blood biochemistry tests, liver biopsy, abdominal ultrasonography, and abdominal CT. During the observation period, no changes in oral medications, antiviral drugs, or other agents were seen (7).

Results:

Serum albumin levels, total protein levels, and Child-Pugh score at 6 months after ABM*i* were significantly improved in patients whose course could be observed for 6 months after ABM*i* (7). Similar improvements were also seen in 9 patients whose course could be observed for 15 months (Fig. 2). We had treated 24 patients as of October 2009, and no particular problems with occurrence of adverse events were encountered (15). Additional trials of the ABM*i* therapy we developed have been conducted with 6 patients at Yamagata University (conducted jointly with a Yamagata University team) and 10 patients at Yonsei University in South Korea (16). These results of our multicenter clinical trials are gradually demonstrating the safety and efficacy of ABM*i* therapy and therapy using autologous bone marrow cells.

4. Conclusions

Reports to date on regenerative and cell therapies using bone marrow (stem) cells for liver cirrhosis include not only those on our ABM*i* therapy (7, 15), but also reports from India on the effectiveness of peripheral administration of bone marrow stem cells (17, 18). Lyra et al. in Brazil also reported the feasibility and safety of autologous bone marrow cell infusion through not a peripheral vein but a hepatic artery for chronic liver disease patients waiting liver transplantation (19, 20). Moreover, Kharaziha et al. showed liver function improvements after administration of autologous mesenchymal stem cells (21). Issues to be investigated in the future include identification of cells showing treatment effects from bone marrow cell fractions and clarification of the mechanisms of such actions. When cells with liver regeneration and restorative activity can be isolated from small amounts of bone marrow fluid, cultured, and then re-administered, the indications would be able to be expanded so that collection of bone marrow fluid would no longer need to be performed under general anesthesia. However, safety evaluation guidelines for cultured cells are needed when autologous marrow-derived cultured cells are used in patients, and a system conforming to SOP at a cell-processing center with GMP grade is essential. In the future, based on liver-function improvement effects from administration of bone marrow (stem) cells for cirrhosis that have been confirmed to date, new treatment methods using less invasive bone marrow-derived cultured cells will need to be developed.

Acknowledgments

This study was supported by Grants-in-Aid for scientific research from the Japan Society for the Promotion of Science, Ministry of Health, Labour, and Welfare, the Knowledge Cluster Initiative, and Japan Science and Technology Agency.

References

1 Alison MR, Poulsom R, Jeffery R, Dhillon AP, Quaglia A, Jacob J, et al. Hepatocytes from non-hepatic adult stem cells. Nature. 2000;406:257.
2 Theise ND, Nimmakayalu M, Gardner R, Illei PB, Morgan G, Teperman L, et al. Liver from bone marrow in humans. Hepatology. 2000;32:11–16.
3 Houlihan DD, Newsome PN. Critical review of clinical trials of bone marrow stem cells in liver disease. Gastroenterology. 2008; 135:438–450.
4 Terai S, Sakaida I, Yamamoto N, Omori K, Wratanabe T, Ohata S, et al. An in vivo model for monitoring trans-differentiation of bone marrow cells into functional hepatocytes. J Biochem. 2003; 134:551–558
5 Terai S, Sakaida I, Nishina H, Okita K. Lesson from the GFP/CCl4 model – translational research project: the development of cell therapy using autologous bone marrow cells in patients with liver cirrhosis. J Hepatobiliary Pancreat Surg. 2005;12:203–207.
6 Sakaida I, Terai S, Yamamoto N, Aoyama K, Ishikawa T, Nishina H, et al. Transplantation of bone marrow cells reduces CCl4-induced liver fibrosis in mice. Hepatology. 2004;40:1304–1311.
7 Terai S, Ishikawa T, Omori K, Aoyama K, Marumoto Y, Urata Y, et al. Improved liver function in patients with liver cirrhosis after autologous bone marrow cell infusion therapy. Stem Cells. 2006; 24:2292–2298.
8 Gordon MY, Levicar N, Pai M, Bachellier P, Dimarakis I, Al-Allaf F, et al. Characterization and clinical application of human CD34+ stem/progenitor cell populations mobilized into the blood by granulocyte colony-stimulating factor. Stem Cells. 2006;24:1822–1830.
9 Levicar N, Pai M, Habib NA, Tait P, Jiao LR, Marley SB, et al. Long-term clinical results of autologous infusion of mobilized adult bone marrow derived CD34+ cells in patients with chronic liver disease. Cell Prolif. 2008;41:115–125.
10 am Esch JS 2nd, Knoefel WT, Klein M, Ghodsizad A, Fuerst G, Poll LW, et al. Portal application of autologous CD133+ bone marrow cells to the liver: a novel concept to support hepatic regeneration. Stem Cells. 2005;23:463–470.
11 Furst G, Schulte am Esch J, Poll LW, Hosch SB, Fritz LB, Klein M, et al. Portal vein embolization and autologous CD133+ bone marrow stem cells for liver regeneration: initial experience. Radiology. 2007;243:171–179.
12 Ishikawa T, Terai S, Urata Y, Marumoto Y, Aoyama K, Sakaida I,

et al. Fibroblast growth factor 2 facilitates the differentiation of transplanted bone marrow cells into hepatocytes. Cell Tissue Res. 2006;323:221–231.

13 Omori K, Terai S, Ishikawa T, Aoyama K, Sakaida I, Nishina H, et al. Molecular signature associated with plasticity of bone marrow cell under persistent liver damage by self-organizing-map-based gene expression. FEBS Lett. 2004 3;578:10–20.

14 Yokoyama Y, Terai S, Ishikawa T, Aoyama K, Urata Y, Marumoto Y, et al. Proteomic analysis of serum marker proteins in recipient mice with liver cirrhosis after bone marrow cell transplantation. Proteomics. 2006;6:2564–2570.

15 Terai S, Sakaida I. Current status of autologous bone marrow cell infusion therapy for liver cirrhosis patients. Hepatol Res. 2008;38(s1The 6 Japan Society of Hepatology Single Topic Conference: Liver Failure: Recent Progress and Pathogenesis to Management. 28-29 September 2007, Iwate, Japan):S72–S75.

16 Kim JK, Park YN, Kim JS, Park MS, Paik YH, Seok JY, et al. Autologous bone marrow infusion activates the progenitor cell compartment in patients with advanced liver cirrhosis. Cell Transplant. 2010;19:1237–1246.

17 Mohamadnejad M, Alimoghaddam K, Mohyeddin-Bonab M, Bagheri M, Bashtar M, Ghanaati H, et al. Phase 1 trial of autologous bone marrow mesenchymal stem cell transplantation in patients with decompensated liver cirrhosis. Arch Iran Med. 2007; 10:459–466.

18 Mohamadnejad M, Namiri M, Bagheri M, Hashemi SM, Ghanaati H, Zare Mehrjardi N, et al. Phase 1 human trial of autologous bone marrow-hematopoietic stem cell transplantation in patients with decompensated cirrhosis. World J Gastroenterol. 2007;13: 3359–3363.

19 Lyra AC, Soares MB, da Silva LF, Fortes MF, Silva AG, Mota AC, et al. Feasibility and safety of autologous bone marrow mononuclear cell transplantation in patients with advanced chronic liver disease. World J Gastroenterol. 2007;13:1067–1073.

20 Lyra AC, Soares MB, da Silva LF, Braga EL, Oliveira SA, Fortes MF, et al. Infusion of autologous bone marrow mononuclear cells through hepatic artery results in a short-term improvement of liver function in patients with chronic liver disease: a pilot randomized controlled study. Eur J Gastroenterol Hepatol. 2010; 22:33–42.

21 Kharaziha P, Hellstrom PM, Noorinayer B, Farzaneh F, Aghajani K, Jafari F, et al. Improvement of liver function in liver cirrhosis patients after autologous mesenchymal stem cell injection: a phase I-II clinical trial. Eur J Gastroenterol Hepatol. 2009;2: 1199–1205.

Hepatology Research

Hepatology Research 2011; **41**: 463–474 doi: 10.1111/j.1872-034X.2011.00784.x

Original Article

Splenectomy reduces fibrosis and preneoplastic lesions with increased triglycerides and essential fatty acids in rat liver cirrhosis induced by a choline-deficient L-amino acid-defined diet

Toshiyuki Oishi,[1] Shuji Terai,[1] Takuya Iwamoto,[1] Taro Takami,[2] Naoki Yamamoto[1] and Isao Sakaida[1]

[1]*Department of Gastroenterology and Hepatology, Yamaguchi University Graduate School of Medicine, and* [2]*Department of Laboratory, Yamaguchi University Hospital, Ube, Yamaguchi, Japan*

Aim: This study investigated whether splenectomy is of significance in non-alcoholic steatohepatitis (NASH).

Methods: Five-week-old Wistar rats were fed a choline-deficient diet for 8 weeks to create a NASH model. A sham-operation or splenectomy was then performed, and rats were killed 4 weeks later.

Results: Liver fibrosis and liver preneoplastic lesions were significantly reduced in the splenectomy group compared to the sham-operation group, and α-smooth muscle actin (SMA) expression was significantly inhibited (liver fibrosis area: sham 8.63 ± 4.09%, splenectomy 5.45 ± 3.69%, $P < 0.01$; preneoplastic lesion size: sham 6.56 ± 3.68 $\times 10^6$ μm²/cm², splenectomy 4.63 ± 3.27 $\times 10^6$ μm²/cm², $P < 0.05$; the number of preneoplastic lesions: sham 8.33 ± 3.96/cm², splenectomy 5.17 ± 1.80/cm², $P < 0.01$; α-smooth muscle actin-positive area: sham 4.41 ± 2.48%, splenectomy 2.75 ± 1.66%, $P < 0.01$) On the other hand, liver triglycerides and essential fatty acids were significantly increased in the splenectomy group (liver triglycerides: sham 182 ± 35.0 mg/g, splenectomy 230 ± 35.0 mg/g, $P < 0.05$; liver linoleic acid: sham 17.2 ± 4.9 mg/g, splenectomy 23.3 ± 6.9 mg/g, $P < 0.05$; liver α-linolenic acid: sham 118 ± 36.6 μg/g, splenectomy 162 ± 51.4 μg/g, $P < 0.05$). In addition, expressions of hepatic fatty acid metabolism-related genes (e.g. acyl-CoA oxidase, liver carnitine palmitoyl-CoA transferase I, cytochrome P450 4A, long-chain acyl-CoA dehydrogenase and medium-chain acyl-CoA dehydrogenase) were significantly inhibited in the splenectomy group.

Conclusion: These findings suggest that spleen plays an important regulatory role in the fibrosis, preneoplastic lesion and lipid metabolism of liver in a rat choline-deficient L-amino acid model.

Key words: fatty acid metabolism, fibrosis, non-alcoholic steatohepatitis, preneoplastic lesion, splenectomy

INTRODUCTION

NON-ALCOHOLIC STEATOHEPATITIS (NASH) is a disease concept first put forward by Ludwig *et al.* in 1980.[1] Despite the absence of a history of alcohol intake sufficient to cause hepatic dysfunction, the pathogenesis of NASH resembles alcoholic liver disease, with progression from simple fatty liver to steatohepatitis and cirrhosis, and ultimately hepatocarcinogenesis.[1] The prevalence of NASH throughout the world is currently increasing. In regard to the etiology of NASH, the two-hit theory proposed by Day *et al.* is currently the most supported theory, stating that fatty liver develops (first hit), followed by the transition to steatohepatitis (second hit).[2] However, the specific mechanisms underlying NASH remain unclear. The first hit of fatty liver is currently thought to develop against a background of so-called metabolic syndrome, with hypertension, dyslipidemia and glucose intolerance, followed by progression to NASH due to some as-yet unknown etiological factor.[2] In addition, NASH can progress to cirrhosis, and ultimately to hepatocellular carcinoma (HCC).

Correspondence: Associate Professor Shuji Terai, Department of Gastroenterology and Hepatology, Yamaguchi University Graduate School of Medicine, 1-1-1 Minami-Kogushi, Ube, Yamaguchi 755-8505, Japan. Email: terais@yamaguchi-u.ac.jp
Received 1 December 2010; revision 9 January 2011; accepted 18 January 2011.

On the other hand, cirrhotic patients occasionally present with hypersplenism, which can result in peripheral cytopenia. Severe peripheral cytopenia may act as a contraindication for aggressive but effective novel therapies, such as interferon therapy or anticancer therapy against HCC with newly developed anticancer drugs, modernized hepatic resection or transplantation.[3] In such cases of hypersplenism, surgical splenectomy is often performed, and postoperative improvements in liver function have been reported.[4,5] Moreover, improved liver fibrosis following splenectomy has been reported in basic research. With regard to underlying mechanisms, splenic-derived transforming growth factor (TGF)-β1, which is thought to stimulate liver fibrosis, may be removed by splenectomy,[6] hepatic tumor necrosis factor (TNF)-α expression may be increased[7] and increased platelet counts may reduce liver fibrosis.[8] Thus, in both basic and clinical studies, splenectomy has been reported to possibly improve liver fibrosis.

Conversely, worsening lipid metabolism due to splenectomy has occasionally been reported. Specifically, rabbits fed a high-cholesterol (high-fat) diet showed decreased high-density lipoprotein cholesterol (HDL-C), increased total cholesterol and triglyceride (TG), and promotion of atherosclerotic changes in the aorta after splenectomy.[9] In addition, rats fed a normal or high-fat diet showed decreased HDL-C and increased TG with splenectomy.[10] In a group of rats fed a normal diet or high-cholesterol diet with subtotal splenectomy, correction of dyslipidemia was reported.[11] In other words, splenectomy may worsen lipid metabolism.

Although the specific etiology of NASH remains unclear, the mechanisms that appear to be involved in the development of this pathology suggest that both fibrosis and lipid metabolism in the liver as factors involved in NASH. However, no studies appear to have described the effects of splenectomy in NASH. This study therefore used a rat choline-deficient L-amino acid (CDAA) diet model (rat steatosis-fibrosis model), as an animal model of NASH,[12,13] to investigate the significance of splenectomy in NASH. We report herein that although splenectomy increased liver TG and essential fatty acids, liver fibrosis and development of preneoplastic lesions were reduced.

METHODS

Animals

MALE WISTAR RATS (5 weeks old, weight 100–120 g; Nippon SLC, Shizuoka, Japan) were quarantined for 1 week, then housed in a room under controlled temperature (25°C), humidity (61–69%) and lighting (12 h light, 12 h dark). Ad libitum access to food and tap water was provided throughout the study period.

Experimental protocol

Rats were divided into two groups: a sham-operation group ($n = 7$) and a splenectomy group ($n = 7$). All rats were fed a CDAA diet for 12 weeks. Eight weeks after beginning the CDAA diet (at 13 weeks old), either a sham-operation (laparotomy and laparorrhaphy without splenectomy) or splenectomy were performed. Four weeks after surgical interventions (at 17 weeks old), all rats were killed. From the start to completion of the study, bodyweight was measured every 4 weeks. At the time of either splenectomy (13 weeks old) or death (17 weeks old), the spleen was weighed.

In addition, we created two normal diet groups: a sham-operation normal diet group ($n = 6$) and a splenectomy normal diet group ($n = 6$). These rats were fed a normal diet from the start to completion of the study. Either a sham-operation or splenectomy were performed at 13 weeks old and all were killed at 17 weeks old.

Measurement of serum markers

Blood samples (5 mL) were obtained from the portal vein at the time of death. White blood cells (WBC), red blood cells (RBC), hemoglobin (Hb) and platelets (Plt) were measured using a KX-21 NV automatic cell counter (Sysmex, Kobe, Japan). Total protein (TP), total bilirubin (T-bil), albumin (Alb), alanine aminotransferase (ALT), aspartate aminotransferase (AST), total cholesterol (T-Cho), TG and HDL-C were measured using an automated analyzer for clinical chemistry (SPOTCHEM EZ SP-4430; Arkray, Kyoto, Japan). TGF-β1 was measured using Immunoassay (enzyme-linked immunosorbent assay; R&D Systems, Minneapolis, MN, USA).

Measurement of triacylglycerol content and fatty acid fractionation in liver tissue

During the 12-week experiment, triacylglycerol content and fatty acid fractionation in liver tissue were measured in all groups. Triacylglycerol in liver tissue was extracted using the method described by Folch *et al.*[14] Fatty acid fractionation in liver tissue was measured using gas chromatography with a flame ionization detector (FID) (GC-17A; Shimadzu, Kyoto, Japan).

Histopathological and immunohistochemical examination

In all experiments, sections (3-μm thick) of the right lobe of all rat livers were fixed in 4% paraformaldehyde phosphate buffer solution, then embedded in paraffin and processed for Sirius-red and immunohistochemical staining. For immunohistochemical analysis, the Vectastain ABC kit (Vector Laboratories, Burlingame, CA, USA) was used to identify anti-α-smooth muscle actin (α-SMA) (dilution 1:300; Abcam, Cambridge, MA, USA), anti-TGF-β1- (dilution 1:100; Santa Cruz Biotechnology, Santa Cruz, CA, USA) and placental-form glutathione *S*-transferase (GST-P)-positive lesions (dilution 1:1000; MBL, Nagoya, Japan) (as preneoplastic lesions) using the avidin–biotin–peroxidase complex method.[15] To estimate Sirius-red-, α-SMA- and TGF-β1-positive areas, MetaMorph software was used for computerized image analysis at ×40 magnification. One section from each liver were prepared for Sirius-red staining, α-SMA and TGF-β1 immunostaining and 10 randomly selected different areas were analyzed per specimen. Positive areas were expressed as the percentage of the total area of the specimen. Three sections from each liver were prepared for GST-P immunostaining. Using a HS all-in-one fluorescence microscope (BZ-9000; Keyence, Osaka, Japan), the section area and preneoplastic lesion area (GST-P-positive area) of each sample were determined. Based on these values, preneoplastic lesion frequency among individuals, and GST-P-positive area per 1-cm^2 section and the number of GST-P-positive lesions per 1-cm^2 section were determined. Data were then compared between groups.

Real-time reverse transcription polymerase chain reaction (RT–PCR) analysis

Total RNA was extracted from each liver using with TRIzol reagent (Invitrogen, Carlsbad, CA, USA) according to the instructions from the manufacturer. Synthesis of cDNA was performed using purified RNA plus random hexamers and the Transcriptor First Strand cDNA synthesis kit (Roche, Indianapolis, IN, USA). All cDNA was stored at −20°C for PCR. Real-time PCR was performed in 20 μL of reaction solution containing 2× Fast SYBR Green Master Mix (Applied Biosystems, California, CA, USA), corresponding primer, sample DNA and d-water. The cycle for PCR was as follows: 1 cycle of 95°C for 20 s; 40 cycles of 3 s at 95°C and 30 s at 60°C; and 1 cycle of 95°C for 15 s, 60°C for 1 min and 95°C for 15 s. Reactions were performed in a Step One Plus real-time PCR system (Applied Biosystems) and amounts of all mRNA were quantified using StepOne ver. 2.1 software (Applied Biosystems). Glyceraldehyde-3-phosphate dehydrogenase (GAPDH) was used as an internal control. For GAPDH and α-SMA, primer sequences were as described by Tajima *et al.*[16] For acyl-coenzyme A oxidase (ACO), liver carnitine palmitoyl-coenzyme A transferase I (L-CPTI), cytochrome P450 4A (CYP4A), long-chain acyl-coenzyme A dehydrogenase (LCAD), medium-chain acyl-coenzyme A dehydrogenase (MCAD), peroxisome proliferator-activated receptor (PPAR)-α, fatty acid synthase (FAS) and sterol regulatory element-binding protein (SREBP)-1c, primer sequences were the same as used by Ringseis *et al.*[17]

Protein extraction and western blotting

Liver samples were obtained from the sham-operation group and splenectomy group. Liver samples (~40 mg) were homogenized in 1 mL of cell lysis buffer (Cell Signaling Technology, Beverly, MA, USA) and a Complete Mini (Roche Diagnostic, Pleasanton, CA, USA) and then were centrifuged. The supernatant represented the whole protein. Next, 40 μg of protein sample was mixed with the same volume of loading buffer (5% 2-mercaptoethanol and 95% Laemmli Sample Buffer [Bio-Rad Laboratories, Hercules, CA, USA]), heated for 3 min at 100°C and separated on 10% sodium dodecylsulfate polyacrylamide gel electrophoresis (SDS-PAGE). Separated bands were transferred to an Immobilon-P transfer membrane (Millipore, Billerica, MA, USA), followed by blocking of the membranes for 1 h with blocking buffer (0.1% Tween-20 [Wako Pure Chemical Industries, Osaka, Japan]), 0.2% I-Block reagent (Tropix, Bedford, MA, USA), and 1 mM Tris-HCl buffer (pH 7.5; Invitrogen). Membranes were then washed with washing buffer (0.1% Tween-20, 1 mM Tris-HCl buffer [pH 7.5]), and incubated for 1 h at room temperature with primary antibodies against α-SMA (Abcam) and β-actin (Abcam) in blocking buffer. After washing, the membrane was incubated for 1 h at room temperature with the appropriate secondary antibodies. Reactive bands were identified using enhanced chemiluminescence (ECL) (Amersham Biosciences, Piscataway, NJ, USA) and autoradiography, in accordance with the instructions from the manufacturers.

Statistical analysis

Statistical significance was determined using Student's *t*-test. Results are presented as the mean ± standard deviation, and differences of $P < 0.05$ were considered significant.

Ethical considerations

This experiment was reviewed by the Committee for Ethics in Animal Experiments of Yamaguchi University Graduate School of Medicine and carried out under the Guidelines for Animal Experiments of Yamaguchi University Graduate School of Medicine and Law no. 105 and Notification no. 6 of the Japanese Government.

RESULTS

Changes in bodyweight

FROM THE START to completion of the study, changes in bodyweight did not differ significantly between groups (Fig. 1a).

Changes in spleen/bodyweight ratios

Spleen/bodyweight ratio at the time of splenectomy (13 weeks old) and spleen/bodyweight ratio at the time of death (17 weeks old) were compared with the spleen/bodyweight ratio in 13-week-old rats fed a normal diet (normal diet group; $n = 8$). Compared to rats on a normal diet, spleen/bodyweight ratios were increased in sham-operation and splenectomized rats at the time of splenectomy and time of death, respectively (normal diet group [13 weeks old], $2.6 \pm 0.4 \times 10^{-3}$; splenectomy [13 weeks old], $5.7 \pm 3.1 \times 10^{-3}$, $P < 0.05$; sham [17 weeks old], $6.4 \pm 1.5 \times 10^{-3}$, $P < 0.01$) (Fig. 1b). Spleen/bodyweight ratios did not differ significantly between the time of splenectomy and the time of death (Fig. 1b).

Blood tests

On blood tests, the splenectomy group showed increased WBC (sham, $6020 \pm 1800/\mu L$; splenectomy, $13\,100 \pm 3900/\mu L$, $P < 0.01$) and increased Plt (sham, $30.3 \pm 8.07 \times 10^4[/\mu L]$; splenectomy group, $39.6 \pm 12.0 \times 10^4[/\mu L]$, $P < 0.05$). No other blood test results showed any significant difference between groups (Table 1 and Fig. 1c).

Histological and immunohistochemical analysis of α-SMA in liver fibrosis

At 4 weeks after sham operation or splenectomy, histological examination of the liver indicated the presence of liver fibrosis in all rats. Liver fibrosis was measured by estimating extracellular matrix deposition using Sirius-red staining. Results showed that splenectomy extensively decreased the Sirius-red-stained area compared with that in sham-operation rats (Fig. 1d,e). Imaging analysis revealed that splenectomy decreased the percentage Sirius-red-positive area compared with sham-operated rats (sham, $8.63 \pm 4.09\%$; splenectomy, $5.45 \pm 3.69\%$, $P < 0.01$) (Fig. 1f).

Activated hepatic stellate cells, which express α-SMA protein, showed marked proliferation in the livers of sham-operated rats (Fig. 2a). On the other hand, splenectomy groups showed extensively decreased α-SMA-positive areas (Fig. 2b). Quantitative analysis showed that splenectomy significantly reduced the percentage area of α-SMA-positive cells compared with that in the sham-operated group (sham, $4.41 \pm 2.48\%$; splenectomy, $2.75 \pm 1.66\%$, $P < 0.01$) (Fig. 2c).

Western blotting analysis of α-SMA protein in liver

To confirm the inhibitory effect of splenectomy on the activation of hepatic stellate cells, we measured expression of α-SMA protein in the liver by western blot analysis. The splenectomy group showed reduced liver expression of α-SMA protein, compared with the sham-operated group (Fig. 2d).

Real-time RT–PCR analysis of α-SMA mRNA in liver

To confirm the inhibitory effects of splenectomy on activation of hepatic stellate cells, we measured liver expression of α-SMA mRNA by real-time RT–PCR. Livers from the splenectomy group showed reduced expression of α-SMA mRNA, compared with the sham-operated group (sham, 2.12 ± 0.93 [ratio]; splenectomy, 1.18 ± 0.42 [ratio], $P < 0.05$) (Fig. 2e).

Immunohistochemical analysis of TGF-β1 expression in liver fibrosis

Transforming growth factor-β1 expression was also analyzed by immunostaining (Fig. 3a). Splenectomy dramatically reduced TGF-β1 expression (Fig. 3b), and decreased TGF-β1-positive areas in the liver (sham, $6.68 \pm 2.52\%$; splenectomy, $4.21 \pm 2.54\%$, $P < 0.01$) (Fig. 3c), despite no significant difference in plasma TGF-β1 levels between the splenectomy group and the sham-operated group (Fig. 1c).

Effect of splenectomy on GST-P-positive lesions

Preneoplastic lesion (GST-P-positive lesion) frequency among individuals in both groups was 100% (Fig. 3d). However, GST-P-positive area per 1-cm^2 section and the number of GST-P-positive lesions per 1-cm^2 section were significantly decreased in the splenectomy group compared to the sham-operated group (size: sham,

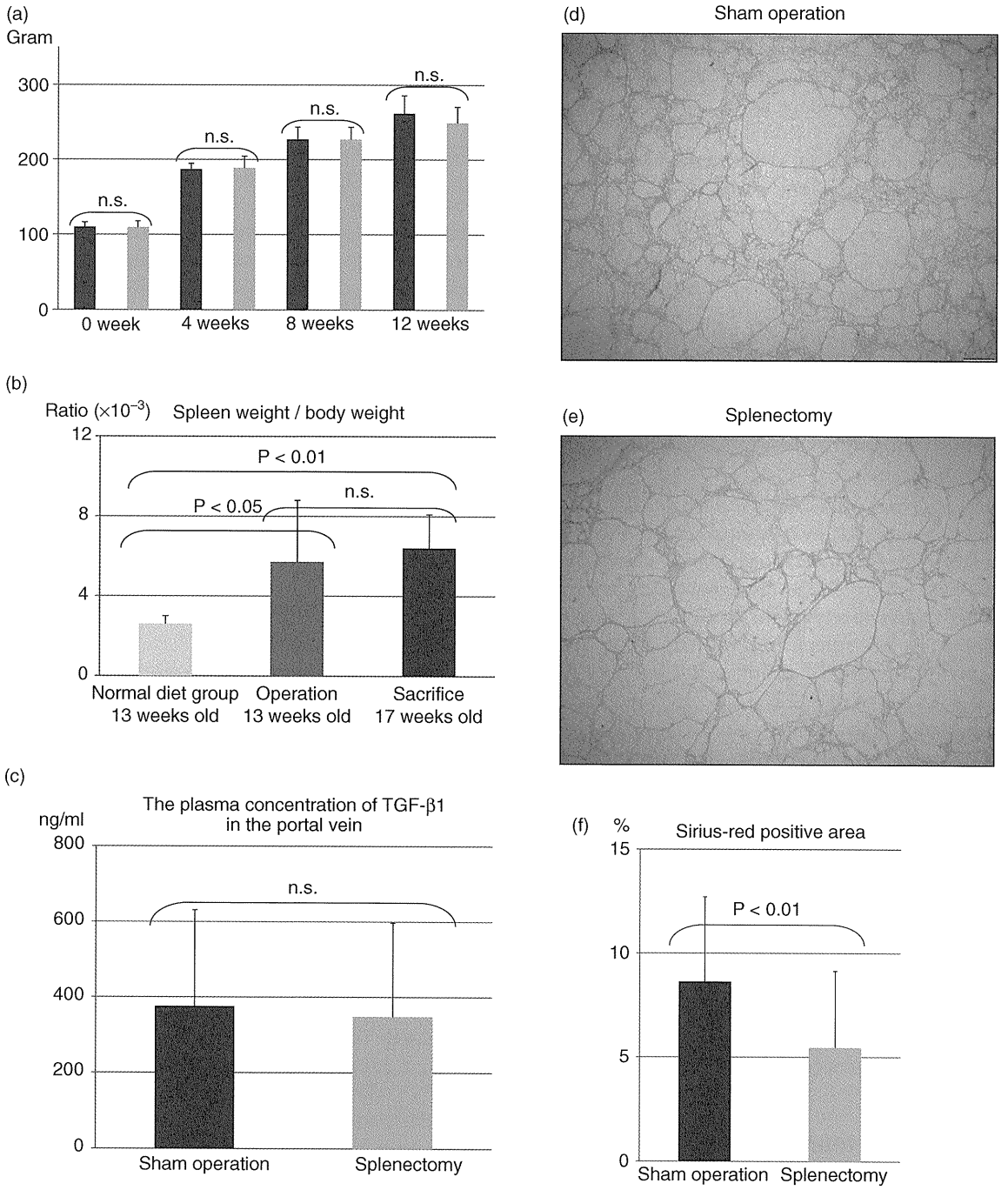

Figure 1 Change in bodyweight from the start to completion of the study (a). Spleen weight/bodyweight ratio (b). The plasma concentration of transforming growth factor (TGF)-β1 in the portal vein (c). Paraffin-embedded liver sections from sham operation, splenectomy rats were performed Sirius-red staining (d,e) (original magnification ×40). Image analysis of Sirius-red-positive areas (f). Data are means ± standard deviation. n.s., no significant difference.

Table 1 Effect of splenectomy on serum markers

	Sham operation	Splenectomy	*P*-value
TP (g/dL)	3.4 ± 0.6	3.9 ± 0.6	n.s.
Alb (g/dL)	1.7 ± 0.36	1.7 ± 0.40	n.s.
T-bil (mg/dL)	0.3 ± 0.1	0.3 ± 0.1	n.s.
ALT (IU/L)	146 ± 62.0	152 ± 65.3	n.s.
AST (IU/L)	294 ± 53.2	330 ± 76.9	n.s.
WBC (/μL)	6 020 ± 1 800	13 100 ± 3 900	<0.01
RBC (/μL)	$617 \pm 34.3 \times 10^4$	$591 \pm 84.0 \times 10^4$	n.s.
Hb (g/dL)	10 ± 0.44	10 ± 10	n.s.
Plt (/μL)	$30.3 \pm 8.07 \times 10^4$	$39.6 \pm 12.0 \times 10^4$	<0.05
T-Cho (mg/dL)	50 ± 0	50 ± 0	n.s.
TG (mg/dL)	41 ± 21	29 ± 9.0	n.s.
HDL-C (mg/dL)	15 ± 3.5	13 ± 5.3	n.s.

Serum markers were measured as described in the text.
Data are means ± standard deviation.
Alb, albumin; ALT, alanine aminotransferase; AST, aspartate aminotransferase; Hb, hemoglobin; HDL-C, high-density lipoprotein cholesterol; n.s., no significant difference; Plt, platelets; RBC, red blood cells; T-bil, total bilirubin; T-Cho, total-cholesterol; TG, triglyceride; TP, total protein; WBC, white blood cells.

$6.56 \pm 3.68 \times 10^6$ μm²/cm², splenectomy, $4.63 \pm 3.27 \times 10^6$ μm²/cm², $P < 0.05$; number: sham, 8.33 ± 3.96/cm², splenectomy, 5.17 ± 1.80/cm², $P < 0.01$) (Fig. 3e,f).

Analysis of triacylglycerol and fatty acid fractionation in the liver

Splenectomy increased liver levels of triacylglycerol (sham, 182 ± 35.0 mg/g; splenectomy, 230 ± 35.0 mg/g, $P < 0.05$) and essential fatty acids (linoleic acid: sham, 17.2 ± 4.9 mg/g, splenectomy, 23.3 ± 6.9 mg/g, $P < 0.05$; α-linolenic acid: sham, 118 ± 36.6 μg/g, splenectomy, 162 ± 51.4 μg/g, $P < 0.05$) compared to sham operation (Fig. 4a–c).

Expression of fatty acid metabolism genes in the liver

Splenectomy reduced the expression of L-CPTI, ACO, CYP4A, LCAD ($P < 0.05$) and MCAD mRNA ($P < 0.01$) (Fig. 4d–h), but did not influence expression of PPAR-α, FAS or SREBP-1c (Fig. 4i–k). There was no significant difference in the expression of L-CPTI, ACO, CYP4A, LCAD and MCAD mRNA between sham-operation and splenectomy normal diet group (Fig. 5a–e).

DISCUSSION

TRANSFORMING GROWTH FACTOR-β1 is a cytokine that causes activation of hepatic stellate cells and stimulates the production of extracellular matrix,[18] and is a major factor for promoting liver fibrosis. In a previous study using a rat model of liver cirrhosis, TGF-β1, produced by splenic macrophages, was reported to possibly inhibit hepatocyte proliferation in damaged liver. Therefore, in the same model, removal of the enlarged spleen was thought to possibly stimulate regeneration of the damaged liver.[6] One potential mechanism underlying the present results could be increased portal blood flow and changes in intrahepatic blood flow, associated with changes in shunt blood flow[4] and changes in TGF-β1 kinetics due to splenectomy.[6]

With a decrease in TGF-β1 expression by splenectomy in the CDAA diet group, hepatic stellate cell activation was inhibited and liver fibrosis improved. Activated stellate cells, which are detected as α-SMA-positive cells and by the expression of α-SMA messenger RNA, cause severe fibrosis as assessed by the hepatic hydroxyproline content. In our previous study,[19] pig serum pretreatment (injection of pig serum into rats induces stellate cell activation resulting in liver fibrosis without parenchymal cell injury) induces more activated stellate cells in the livers of rats subsequently fed a CDAA diet compared with rats fed the CDAA diet alone. Pre-existing fibrosis induced by the activation of stellate cells with pig serum pretreatment has increased hepatic malondialdehyde (MDA) level in parallel with GST-P-positive lesions. These results indicate that pre-existing fibrosis with the activated stellate cells accelerates the development of preneoplastic lesions in a CDAA diet model, so inhibition of hepatocyte stellate cell activation by splenectomy was probably a contributing factor.

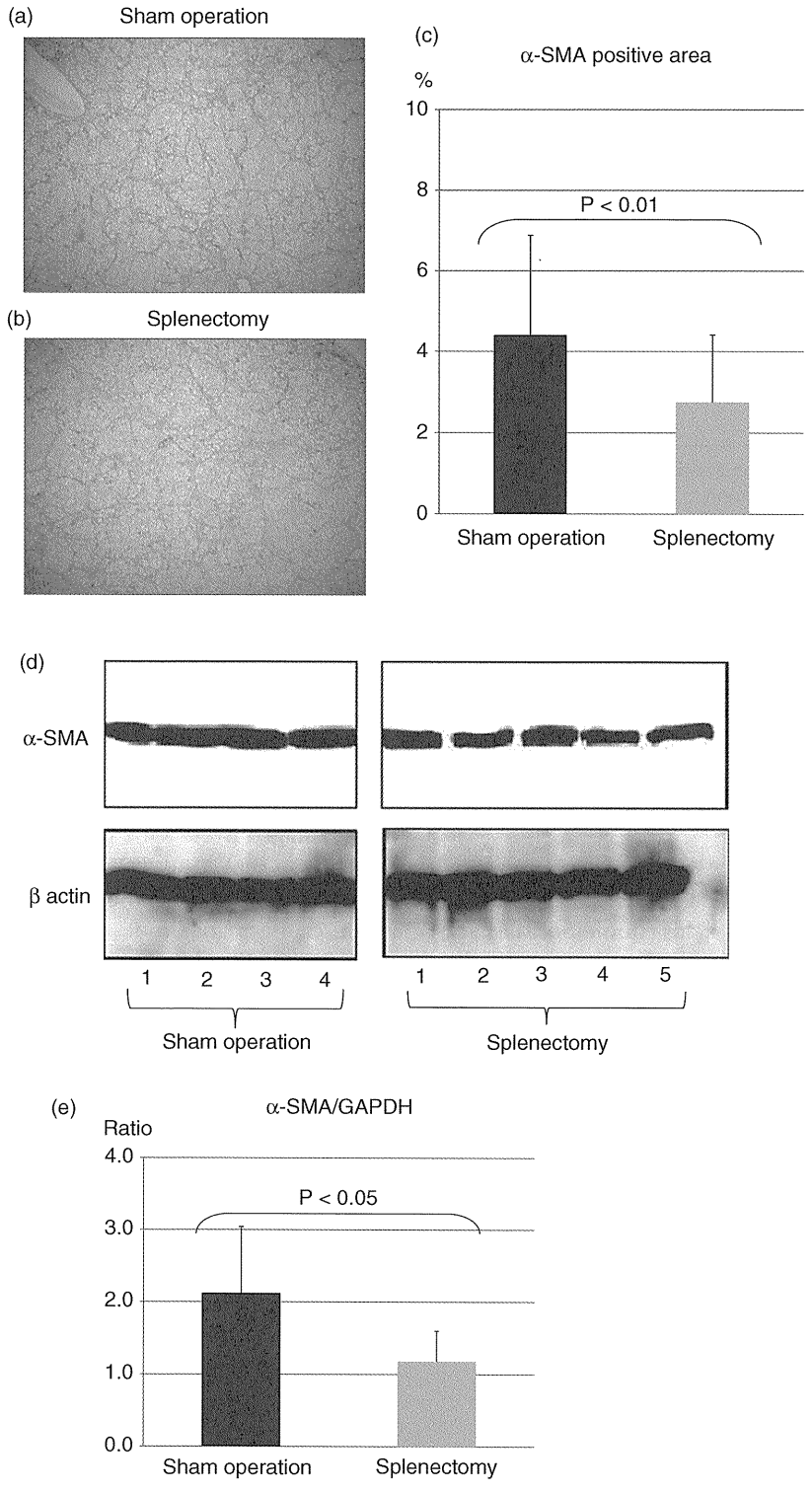

Figure 2 Paraffin-embedded liver sections from sham operation (a) and splenectomy (b) were immunostained for α-smooth muscle actin (α-SMA) (original magnification ×40). Image analysis of α-SMA-positive areas (c). In western blotting, α-SMA expression was inhibited by splenectomy (d). In real-time reverse transcription polymerase chain reaction, mRNA expression of α-SMA was decreased by splenectomy in liver (e). Data are means ± standard deviation. GAPDH, glyceraldehyde 3-phosphate dehydrogenase.

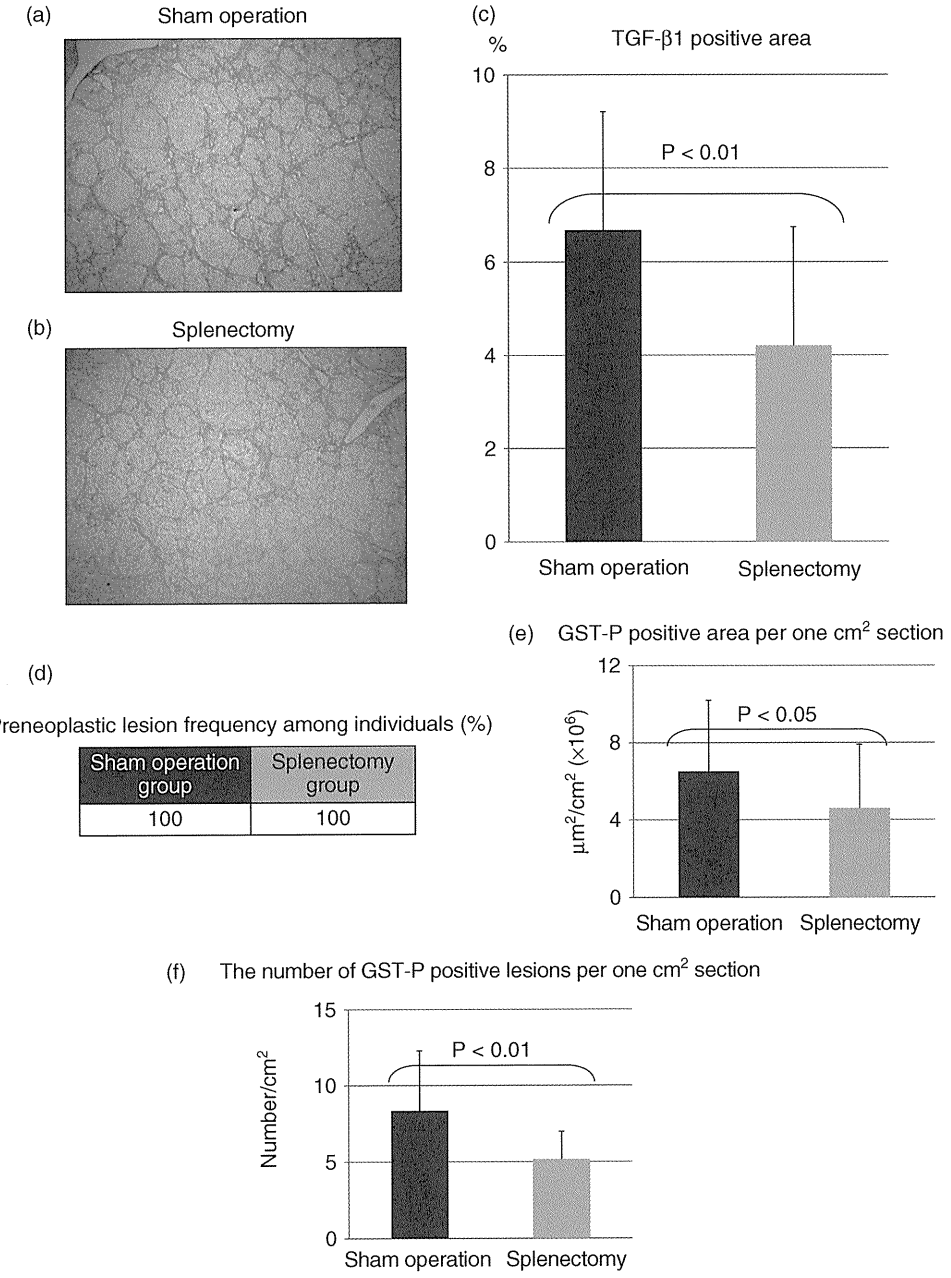

Figure 3 Paraffin-embedded liver sections from sham operation (a) and splenectomy (b) were immunostained for transforming growth factor (TGF)-β1 (original magnification ×40). Image analysis of TGF-β1-positive areas (c). Preneoplastic lesion frequency among individuals (d). Glutathione *S*-transferase (GST-P)-positive area per 1-cm^2 section (e). The number of GST-P-positive lesion per 1-cm^2 section (f). Data are means ± standard deviation.

The mechanism of increased liver fatty acids is thought to be an increase in liver fatty acid synthesis, increased lipid uptake by the liver or decreased liver lipid metabolism. Essential fatty acids are essential for survival of humans and other mammals. These fatty acids cannot be synthesized in the body and must be obtained from the diet.[20,21] Two types of naturally occurring essential fatty acids are used in the body: the ω-6 series derived from *cis*-linoleic acid (LA, 18:2) and the ω-3 series derived from α-linolenic acid (ALA, 18:3).

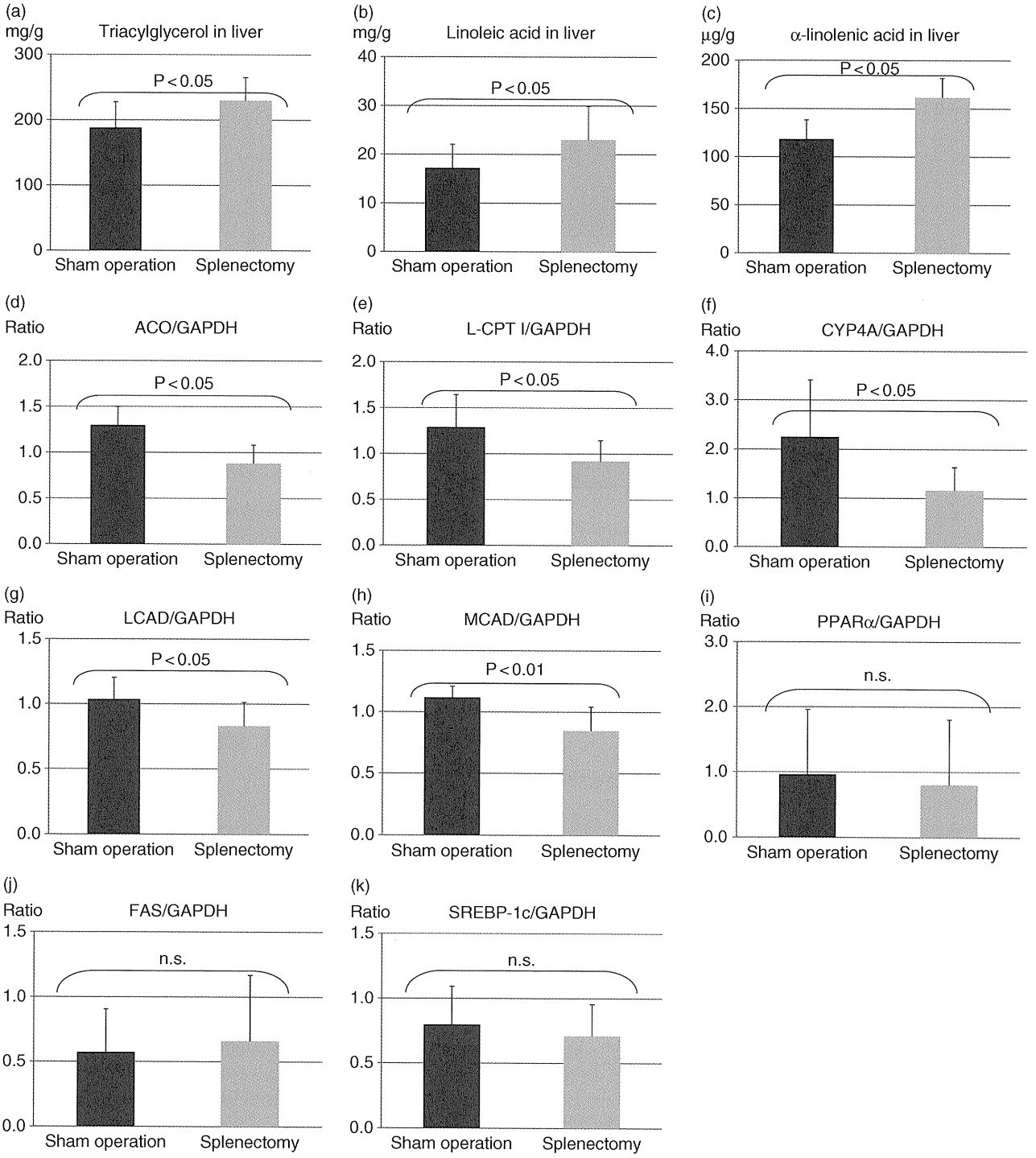

Figure 4 Liver TG (a) and linoleic acid (b) and α-linolenic acid in liver (c). mRNA expression of ACO (d), L-CPTI (e), CYP4A (f), LCAD (g), MCAD (h), PPAR-α (i), FAS (j) and SREBP-1c (k) in liver between sham operation and splenectomy group. Data are means ± standard deviation. ACO, acyl-coenzyme A oxidase; CYP4A, cytochrome P450 4A; FAS, fatty acid synthase; GAPDH, glyceraldehyde 3-phosphate dehydrogenase; LCAD, long-chain acyl-coenzyme A dehydrogenase; L-CPTI, liver carnitine palmitoyl-coenzyme A transferase I; MCAD, medium-chain acyl-coenzyme A dehydrogenase; n.s., no significant difference; PPAR-α, peroxisome proliferator-activated receptor-α; SREBP-1c, sterol regulatory element-binding protein-1c; TG, triglyceride.

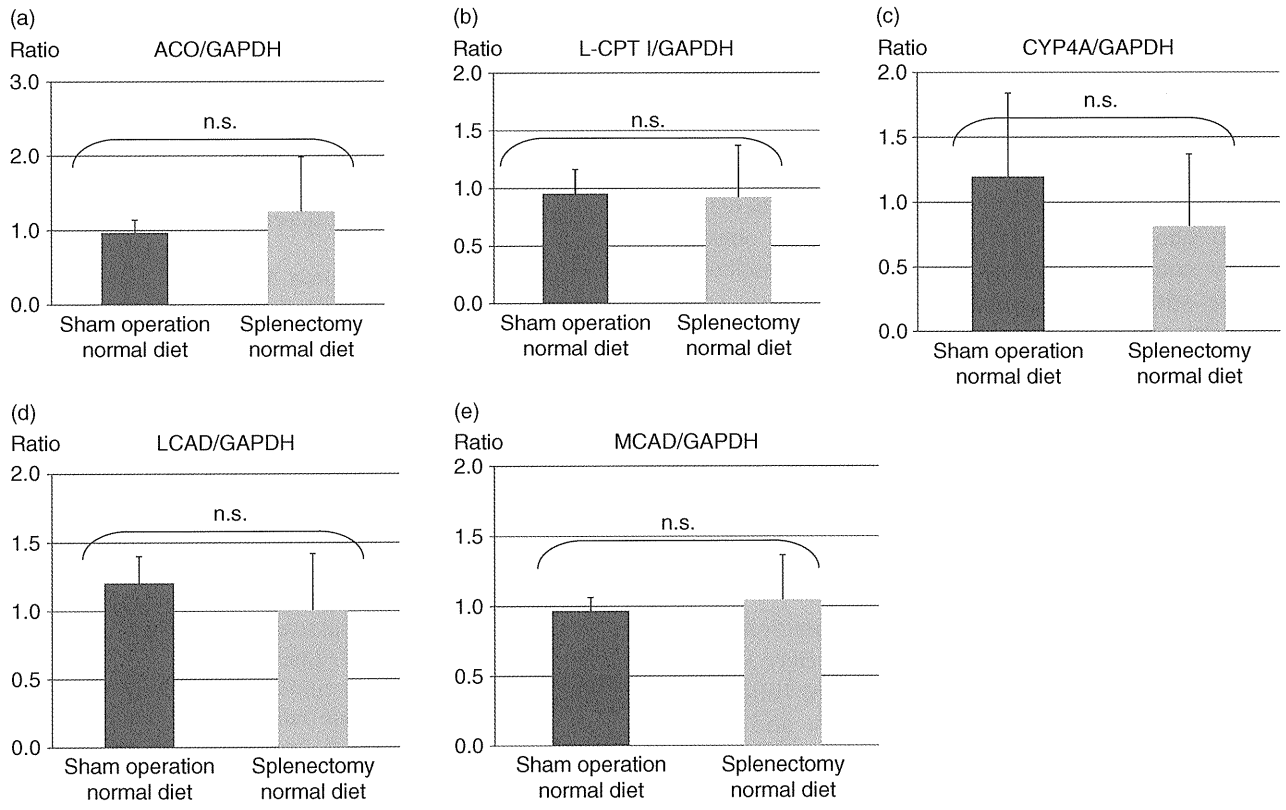

Figure 5 mRNA expression of ACO (a), L-CPTI (b), CYP4A (c), LCAD (d) and MCAD (e) in liver between sham operation and splenectomy normal diet group. Data are means ± standard deviation. n.s., no significant difference. ACO, acyl-coenzyme A oxidase; CYP4A, cytochrome P450 4A; GAPDH, glyceraldehyde 3-phosphate dehydrogenase; LCAD, long-chain acyl-coenzyme A dehydrogenase; L-CPTI, liver carnitine palmitoyl-coenzyme A transferase I; MCAD, medium-chain acyl-coenzyme A dehydrogenase; n.s., no significant difference.

From our results, exacerbation of fatty liver changes is thus likely caused by decreases in fatty acid metabolism. In other words, decreased liver fatty acid metabolism in the splenectomy group would increase liver essential fatty acids, and thus increase liver TG.

As our model is an undernutrition steatosis model,[12,13] no significant differences were seen between groups in terms of blood lipids. However, according to previous reports using normal and high-fat diets, splenectomy may worsen blood lipid metabolism.[9–11] This may also have developed due to an exacerbation of fatty liver changes by splenectomy.

It remains unclear the amount of essential fatty acids in the liver and the working. Our result showed that the quantity of essential fatty acids was proportional to TG and was inverse proportional to fibrosis area in the end-stage of NASH. These results suggest that the quantity of essential fatty acid in the liver decreases when NASH progresses to cirrhosis.

As detailed studies on NASH etiology and pathogenesis have not yet been conducted, no clear statement can be made about whether splenectomy can improve NASH pathogenesis. However, our study focusing on and comparing liver fibrosis and preneoplastic lesions found that both were clearly reduced by splenectomy. In cases of liver fibrosis due to NASH, splenectomy may improve liver fibrosis. In addition, in humans, the incidence of HCC in NASH over a 19.5-year observation period has been reported as 0–2.8%.[22–25] Splenectomy has potential as a therapy to reduce this incidence.

The past human study[26] showed that older age and advanced fibrosis were important risk factors for HCC, and that the steatosis in NASH patients without HCC was severer than that with HCC. These results suggest that the quantity of TG in the liver decreases when NASH progresses to cirrhosis. In other words, it is suggested that liver fibrosis decreases but steatosis is severer

when some factors improve NASH in the end stage. It is consistent with our result.

Based on the above, aggressive treatment with splenectomy may be worthwhile in NASH patients in whom symptoms and morbidity are primarily associated with liver fibrosis and cirrhosis as major determinants of prognosis. On the other hand, in NASH patients in whom symptoms and morbidity are due to obesity, poorly controlled lifestyle disease or atherosclerotic disease, which are determinants of the prognosis, splenectomy may exacerbate the lifestyle-related disease, so particular caution must be taken.

In conclusion, these findings suggest that spleen plays an important regulatory role in the fibrosis, preneoplastic lesion and lipid metabolism of liver in a rat CDAA model.

ACKNOWLEDGMENTS

THIS STUDY WAS supported by Grants-in-Aid for scientific research from the Japan Society for the Promotion of Science, Ministry of Health, Labor and Welfare, the Knowledge Cluster Initiative and Japan Science and Technology agency.

REFERENCES

1 Ludwig J, Viggiano TR, McGill DB, Oh BJ. Nonalcoholic steatohepatitis: Mayo Clinic experiences with a hitherto unnamed disease. *Mayo Clin Proc* 1980; **55**: 434–8.
2 Day CP, James OF. Steatohepatitis: a tale of two "hits"? *Gastroenterology* 1998; **114**: 842–5.
3 McCormick PA, Walker S, Benepal R. Hypersplenism is related to age of onset of liver disease. *Ir J Med Sci* 2007; **176**: 293–6. Epub 18 Oct 2007.
4 Murata K, Ito K, Yoneda K, Shiraki K, Sakurai H, Ito M. Splenectomy improves liver function in patients with liver cirrhosis. *Hepatogastroenterology* 2008; **55**: 1407–11.
5 Imura S, Shimada M, Utsunomiya T *et al.* Impact of splenectomy in patients with liver cirrhosis: results from 18 patients in a single center experience. *Hepatol Res* 2010; **40**: 894–900.
6 Akahoshi T, Hashizume M, Tanoue K *et al.* Role of the spleen in liver fibrosis in rats may be mediated by transforming growth factor beta-1. *J Gastroenterol Hepatol* 2002; **17**: 59–65.
7 Murata K, Shiraki K, Sugimoto K *et al.* Splenectomy enhances liver regeneration through tumor necrosis factor (TNF)-alpha following dimethylnitrosamine-induced cirrhotic rat model. *Hepatogastroenterology* 2001; **48**: 1022–7.
8 Watanabe M, Murata S, Hashimoto I *et al.* Platelets contribute to the reduction of liver fibrosis in mice. *J Gastroenterol Hepatol* 2009; **24**: 78–89. Epub 25 Jun 2008.
9 Asai K, Kuzuya M, Naito M, Funaki C, Kuzuya F. Effects of splenectomy on serum lipids and experimental atherosclerosis. *Angiology* 1988; **39**: 497–504.
10 Fatouros M, Bourantas K, Bairaktari E, Elisaf M, Tsolas O, Cassioumis D. Role of the spleen in lipid metabolism. *Br J Surg* 1995; **82**: 1675–7.
11 Paulo DN, Paulo IC, Morais AA *et al.* Is splenectomy a dyslipidemic intervention? Experimental response of serum lipids to different diets and operations. *Microsurgery* 2009; **29**: 154–60.
12 Koteish A, Diehl AM. Animal models of steatosis. *Semin Liver Dis* 2001; **21**: 89–104.
13 Kawaguchi K, Sakaida I, Tsuchiya M, Omori K, Takami T, Okita K. Pioglitazone prevents hepatic steatosis, fibrosis, and enzyme-altered lesions in rat liver cirrhosis induced by a choline-deficient L-amino acid-defined diet. *Biochem Biophys Res Commun* 2004; **315**: 187–95.
14 Folch J, Lees M, Sloane Stanley GH. A simple method for the isolation and purification of total lipides from animal tissues. *J Biol Chem* 1957; **226**: 497–509.
15 Ishigaki N, Yamamoto N, Jin H, Uchida K, Terai S, Sakaida I. Continuos intravenous infusion of atrial natriuretic peptide (ANP) prevented liver fibrosis in rat. *Biochem Biophys Res Commun* 2009; **378**: 354–9. Epub 6 Nov 2008.
16 Tajima K, Terai S, Takami T, Kawaguchi K, Okita K, Sakaida I. Importance of inhibitor of DNA binding/differentiation 2 in hepatic stellate cell differentiation and proliferation. *Hepatol Res* 2007; **37**: 647–55. Epub 6 Jun 2007.
17 Ringseis R, Muschick A, Eder K. Dietary oxidized fat prevents ethanol-induced triacylglycerol accumulation and increases expression of PPARalpha target genes in rat liver. *J Nutr* 2007; **137**: 77–83.
18 Hellerbrand C, Stefanovic B, Giordano F, Burchardt ER, Brenner DA. The role of TGF beta1 in initiating hepatic stellate cell activation in vivo. *J Hepatol* 1999; **30**: 77–87.
19 Sakaida I, Hironaka K, Uchida K, Suzuki C, Kayano K, Okita K. Fibrosis accelerates the development of enzyme-altered lesions in the rat liver. *Hepatology* 1998; **28**: 1247–52.
20 Das UN, Horrobin DF, Begin ME *et al.* Clinical significance of essential fatty acids. *Nutrition* 1988; **4**: 337–42.
21 Das UN. Essential fatty acids: biology and their clinical implications. *Asian Pacific J Pharmacol* 1991; **6**: 317–30.
22 Adams LA, Lymp JF, St Sauver J *et al.* The natural history of nonalcoholic fatty liver disease: a population-based cohort study. *Gastroenterology* 2005; **129**: 113–21.
23 Ekstedt M, Franzén LE, Mathiesen UL *et al.* Long-term follow-up of patients with NAFLD and elevated liver enzymes. *Hepatology* 2006; **44**: 865–73.

24 Ong JP, Pitts A, Younossi ZM. Increased overall mortality and liver-related mortality in non-alcoholic fatty liver disease. *J Hepatol* 2008; **49**: 608–12. Epub 2008 Jul 9.
25 Rafiq N, Bai C, Fang Y *et al.* Long-term follow-up of patients with nonalcoholic fatty liver. *Clin Gastroenterol Hepatol* 2009; **7**: 234–8. Epub 2008 Nov 7.
26 Hashimoto E, Yatsuji S, Tobari M *et al.* Hepatocellular carcinoma in patients with nonalcoholic steatohepatitis. *J Gastroenterol* 2009; **44** (Suppl 19): 89–95. Epub 2009 Jan 16.

Journal of Gastroenterology and Hepatology

JGHF

doi:10.1111/j.1440-1746.2011.07016.x

THERAPEUTIC TARGETS OF ALPD AND CIRRHOSIS

Autologous bone marrow cell infusions suppress tumor initiation in hepatocarcinogenic mice with liver cirrhosis

Masaki Maeda,* Taro Takami,† Shuji Terai* and Isao Sakaida*

*Department of Gastroenterology and Hepatology, Yamaguchi University Graduate School of Medicine, and †Division of Laboratory, Yamaguchi University Hospital, Yamaguchi University School of Medicine, Yamaguchi, Japan

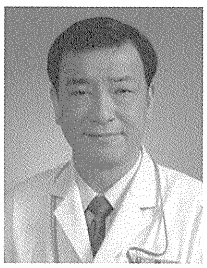

Isao Sakaida

Key words
bone marrow cell, liver cirrhosis, neoplasm, oxidative stress.

Accepted for publication 12 November 2011.

Correspondence
Dr. Taro Takami, Assistant Professor, Division of Laboratory, Yamaguchi University Hospital, 1-1-1 Minami-Kogushi, Ube, Yamaguchi 755-8505, Japan. Email: t-takami@yamaguchi-u.ac.jp

Abstract

We have previously reported the efficacy and safety of autologous bone marrow cell infusion (ABM*i*) therapy for liver cirrhosis patients without hepatocellular carcinoma in a multicenter clinical trial. However, since liver cirrhosis is highly oncogenic, evaluation of the effects of ABM*i* on the mechanisms of hepatocarcinogenesis is of great importance. Therefore, frequent ABM*i* was performed in hepatocarcinogenic mice, and its effects on hepatocarcinogenesis were analyzed. The *N*-nitrosodiethylamine (DEN)/green fluorescent protein (GFP)-carbon tetrachloride (CCl_4) model was developed by administering DEN once, followed by repeated administration of CCl_4 intraperitoneally as for the control group. In the administration (ABM*i*) group, GFP-positive bone marrow cells were infused through a tail vein. The kinetics of hepatocarcinogenesis were evaluated histologically 4.5 months after DEN treatment. At 4.5 months, there was significantly lower incidence of foci and tumors in the ABM*i* group, and they were smaller in number, while their size was almost equal. No GFP-positive tumors were found in ABM*i* livers. Moreover, ABM*i* livers showed significantly reduced liver fibrosis, consistent with significantly lower 8-hydroxy-2′-deoxyguanosine levels, higher superoxide dismutase activity, and increased nuclear translocation of nuclear factor-erythroid 2 p45-related factor 2. These results demonstrate that frequent ABM*i* might contribute to suppressed tumor initiation during stages of hepatocarcinogenesis, consistent with improvements in liver fibrosis and stabilization of redox homeostasis.

Introduction

Hepatocellular carcinoma (HCC) accounts for the fifth largest number of cancer patients worldwide.[1] In Japan, the number of deaths from HCC exceeds 30 000 per year, of which approximately 70% are as a result of persistent hepatitis C virus (HCV) infection. The majority of these patients already have liver cirrhosis (LC).[2] In cases that have progressed to decompensated LC, the only radical treatment available today is still liver transplantation. However, transplants are not widely performed in Japan, due to various problems, including a chronic donor shortage, surgical invasiveness, risk of immunological rejection, and medical costs.

In our developed green fluorescent protein (GFP)/carbon tetrachloride (CCl_4) murine model (the GFP/CCl_4 model), we reported that, in an environment of chronic inflammation, donor-derived bone marrow cells (BMC) engraft along fibers surrounding the portal area and act to degrade existing liver fibrosis by producing matrix metalloproteinase (MMP)-9 and other collagenases, which has led to significant improvements in liver fibrosis, hepatic functions, and survival outcomes.[3–6] In addition, a clinical trial of autologous BMC infusion (ABM*i*) therapy for liver cirrhosis, based on the results of the GFP/CCl_4 model, was started in November 2003,[7] and a multicenter clinical trial (Liver Regeneration with Cell Transplantation study) was started in 2005.[8,9] Kim *et al.* used ABM*i* therapy to treat patients with decompensated hepatitis B virus (HBV)-related LC, and reported elevated serum albumin levels and improved Child-Pugh scores. From the liver biopsies, the mechanism for these effects appeared to be the activation of hepatic progenitor cells.[10] Saito *et al.* also reported the efficacy and safety of ABM*i* therapy for alcoholic LC.[11]

However, while there have been several reports on the effects of autologous BMC on cancer,[12,13] it is unclear whether ABM*i* promotes hepatocarcinogenesis. We therefore performed ABM*i* therapy only on LC patients without concurrent HCC on imaging tests, such as computed tomography. As mentioned earlier, however, LC itself is a cancer risk, and it is widely known that the cancer incidence is particularly high in HCV-related LC patients, at approximately 7% annually.[14–17] Evaluation of how ABM*i* affects hepatocarcinogenesis in LC without concomitant HCC is thus of great importance.

In the present study, the effects of ABM*i* on hepatocarcinogenesis were investigated by preparing new highly-oncogenic cirrhotic mice (the *N*-nitrosodiethylamine [DEN]/GFP-CCl_4 model). In the present study, the results of the analysis showed that ABM*i* does not promote, but rather inhibits hepatocarcinogenesis.

Methods

Mice

GFP-transgenic mice (TgN[β-act-EGFP]Osb) were kindly provided by Masaru Okabe (Genome Research Center, Osaka University, Osaka, Japan). C57BL/6 male mice purchased from Chiyoda SLC (Tokyo, Japan) were properly anesthetized during the experiments. These mice were maintained in specific pathogen-free housing at the Animal Experiment Facility of Yamaguchi University School of Medicine, and cared for in accordance with the animal ethics requirements at Yamaguchi University School of Medicine after approval of the experimental protocol.

Experimental protocol for the DEN/GFP-CCl_4 model

Male mice received a single intraperitoneal injection of 10 μg/g body weight of DEN (Sigma-Aldrich Japan, Tokyo, Japan) at 14 days of age. From 1 month after DEN treatment, the mice were treated with 1 mL/kg body CCl_4 (Wako, Osaka, Japan) dissolved in corn oil (1 : 3), twice a week for 14 weeks. These were used as the control group ($n = 17$). In the administration group (ABM*i*; $n = 23$), GFP-positive BMC were infused biweekly through the tail vein, for a total of five BMC injections, from 2 months after DEN treatment. In this model, 1×10^6 GFP-positive BMC were infused without culture. The kinetics of hepatocarcinogenesis were histologically evaluated 4.5 months after DEN treatment based on the incidence, number, and size of foci and tumors (including adenoma and HCC) (Fig. 1).

Histology and immunohistochemistry

Livers were fixed in 4% formaldehyde overnight at 4°C. Paraffin sections (3 μm thick) were stained with hematoxylin and eosin (H&E) for histological examination and quantification of hepatic lesions graded as foci, adenomas, or carcinoma, as defined previously.[18] The areas occupied by foci or tumor were measured using an Olympus Provis microscope equipped with a CCD camera (Olympus, Tokyo, Japan). The liver fibrosis area was quantified with Sirius red staining using the camera noted above. The Sirius red-stained area, considered the fibrotic area, was assessed by computer-assisted image analysis with MetaMorph software (Universal Imaging, Downingtown, PA, USA) at a magnification of × 40. The mean value of three randomly-selected areas per sample was used as the expressed percentage area of fibrosis. Immunohistochemical staining was performed on formaldehyde-fixed, paraffin-embedded tissue sections using the immunoperoxidase method. In cases of detection of the GFP, normal goat serum (Vector Laboratories, Burlingame, CA, USA) was applied for 20 min and removed. Sections were incubated with rabbit anti-GFP antibody (A11122; Invitrogen, Carlsbad, CA, USA) at a dilution of 1 : 200 overnight at 4°C in a moist chamber. After washing three times in phosphate-buffered saline (PBS) (Nissui Pharmaceutical, Tokyo, Japan), sections were incubated with biotinylated secondary antibody for 1 h at room temperature. The bound antibody was detected using the avidin-biotin complex method staining kit (Vector Laboratories, USA). The goat anti-AFP antibody (SC8108; Santa Cruz Biotechnology, Santa Cruz, CA, USA) at a dilution of 1 : 250 was used for the α-fetoprotein (AFP) protein, rabbit anti-superoxide dismutase 3 antibody (ab81144; Abcam, Cambridge, UK) at a dilution of 1 : 100 was used for the superoxide dismutase (SOD) 3 protein, and rabbit anti-Nrf2 antibody (ab31163; Abcam, UK) at a dilution of 1 : 100 was used for nuclear factor-erythroid 2 p45-related factor 2 (Nrf2) protein. Additionally, double immunofluorescent staining was performed to assess the co-expression of the GFP noted above and SOD3 protein using goat anti-SOD3 antibody (SC3222; Santa Cruz Biotechnology, USA). The secondary antibodies, antirabbit immunoglobulin G (IgG), Alexa Fluor 488 (A11034, Molecular Probes in Life Technologies Japan, Tokyo, Japan) and antigoat IgG, Alexa Fluor 568 (A11077, Molecular Probes in Life Technologies Japan) were each applied at a concentration of 1 : 400 in PBS for 60 min at room temperature. Before attaching the coverslip, DAPI (Dojindo Laboratories, Kumamoto, Japan) was applied for counterstaining to visualize all nuclei in the tissue section. Immunofluorescent liver sections were observed using a Keyence BIOREBO BZ-9000 fluorescence microscope (Keyence Japan, Tokyo, Japan).

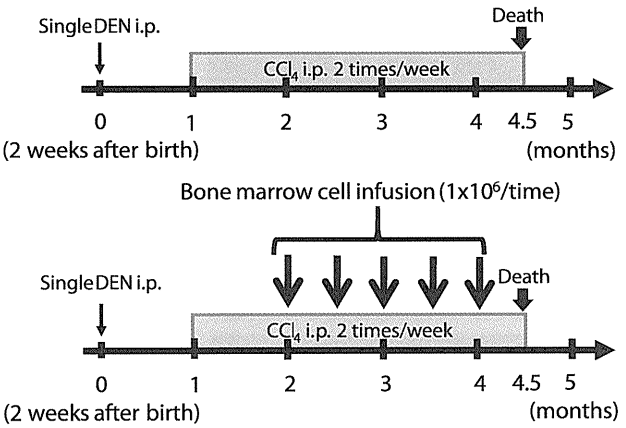

Figure 1 Experimental protocol (the *N*-nitrosodiethylamine [DEN]/green fluorescent protein-carbon tetrachloride [CCl_4] model). Mice received a single injection of DEN at 2 weeks of age. From 1 month after DEN treatment, mice were treated with CCl_4 twice per week. These were used as the control group ($n = 17$). In the administration group (autologous bone marrow cell infusion group, $n = 23$), bone marrow cells (1×10^6/time) were infused biweekly from 2 months after DEN treatment. Kinetics of hepatocarcinogenesis were evaluated histologically 4.5 months after DEN treatment.

8-hydroxy-2′-deoxyguanosine ELISA

The DNA extractor TIS kit (Wako, Japan), which was able to inhibit the oxidation of DNA, was used for the extraction of DNA from 150-mg deep-frozen mouse liver per sample. The 8-hydroxy-2′-deoxyguanosine (8-OHdG) assay preparation reagent set (Wako, Japan), to reduce the variation of the enzyme reaction by

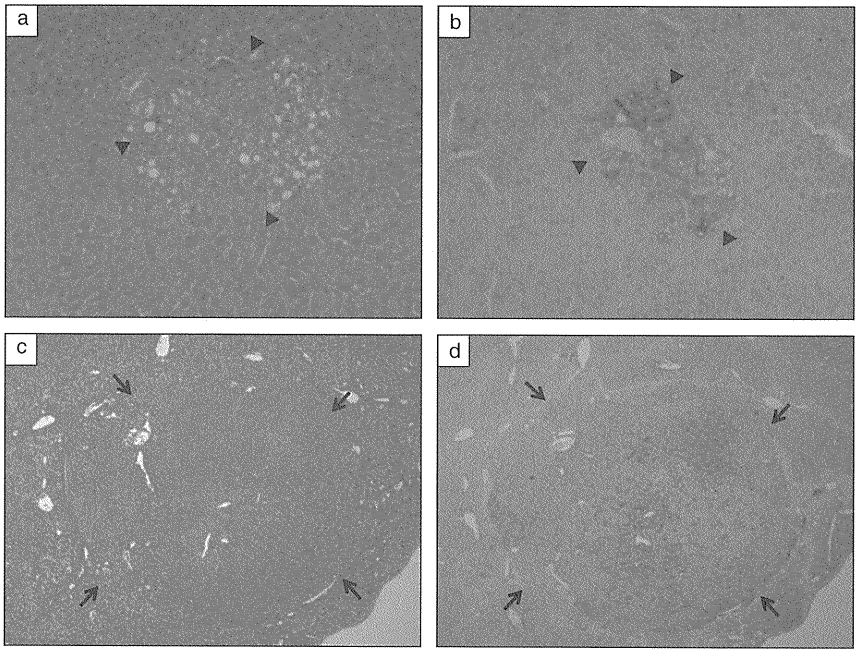

Figure 2 Foci and tumor in murine livers of the autologous bone marrow cell infusion (ABM*i*) group at 4.5 months after *N*-nitrosodiethylamine treatment. (a,b) Foci. Serial sections showing foci from the ABM*i* group with hematoxylin and eosin (H&E) (a), and for α-fetoprotein (AFP) (b) (× 100). Arrowheads show foci. Expression of AFP is upregulated in foci. (c,d) Tumor. Serial sections showing tumors from the ABM*i* group with HE (c) and stain for AFP (d) (× 40). Arrows show tumor. Expression of AFP is also upregulated in the tumor.

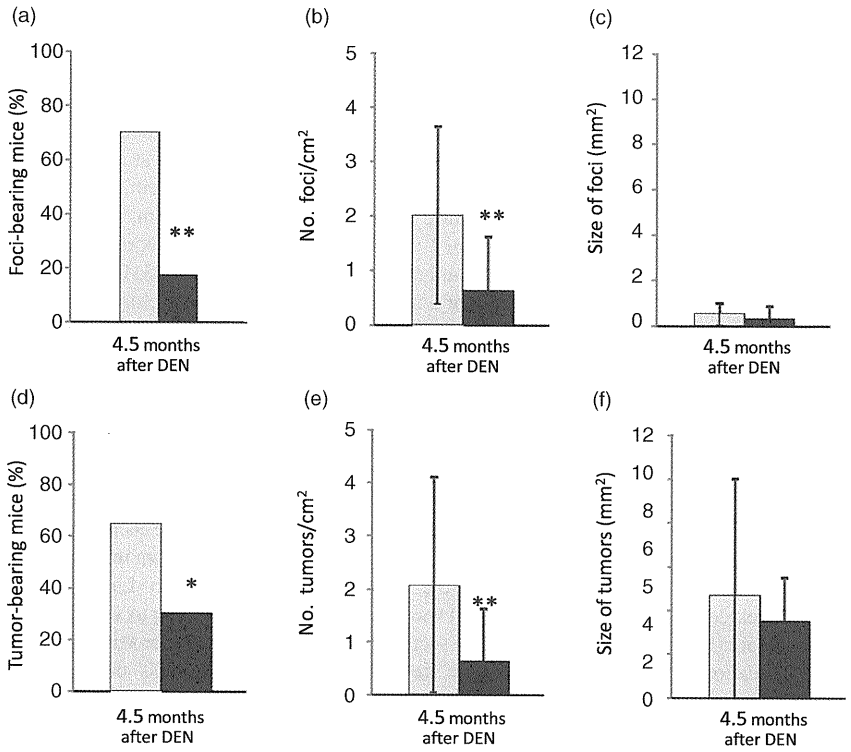

Figure 3 Kinetics of tumor development at 4.5 months after *N*-nitrosodiethylamine (DEN) treatment. (a–c) Foci (d–f) tumor in the control group ($n = 17$) and the autologous bone marrow cell infusion (ABM)/group ($n = 23$) at 4.5 months after DEN treatment. (a,d) Incidence. Columns, percentage (%) of foci- (a) and tumor-(d) bearing mice. (b,e) Multiplicity. Columns, mean number per cm^2 of foci (b) and tumor (e). (c,f) Size. Columns, average size (mm^2) of foci (c) and tumor (f). Bar = standard deviation. $^*P < 0.05$, $^{**}P < 0.01$ compared to the control group. Gray columns = the control group, black columns = the ABM*i* group.

addition of each reagent to the sample DNA, was also used to obtain stable assay results for a marker of oxidant stress. Hepatic 8-OHdG levels were analyzed by the 8-OHdG ELISA assay kit (Japan Institute for the Control of Aging, Shizuoka, Japan); all samples were analyzed in triplicate.

Hepatic SOD activity assay

Deep-frozen liver tissues were homogenized with a cell lysis solution (Thermo Scientific Pierce, Kanagawa, Japan). After 60 min of centrifugation at 78 000 × *g*, aliquots of the obtained supernatant

Journal of Gastroenterology and Hepatology **27** (2012) Suppl. 2; 104–111

were assayed. The total protein concentration was measured by the BCA kit reagent (Thermo Scientific Pierce, Japan). SOD activity was checked using the SOD assay kit-WST (Dojindo Molecular Technologies, Gaithersburg, MD, USA). Briefly, 20 μL of these aliquots were incubated with WST working solution and enzyme working solution containing xanthine, a water-soluble tetrazolium salt, and xanthine oxidase for 20 min at 37°C. The superoxide free radicals generated from the xanthine substrate by xanthine oxidase reduce tetrazolium salt (WST-1) to WST-1 diformazan. SOD in these aliquots inhibits WST-1 reduction as it catalyzes the dismutation of superoxide ions to molecular oxygen and hydrogen peroxide. The reduction of WST-1 was measured by spectrophotometry at 450 nm. All samples were analyzed in triplicate.

Statistical analysis

Statistical significance was determined using the two-tailed Student's *t*-test. Results are presented as the means ± standard deviation, and differences with a *P*-value less than 0.05 were considered significant.

Results

Frequent bone marrow cell infusion suppresses tumor initiation in hepatocarcinogenic mice with liver cirrhosis

Two months after DEN treatment, when the first BMC infusion was performed, no focal lesions were seen in murine livers (data not shown). Then, 4.5 months after DEN treatment, when the kinetics of hepatocarcinogenesis were evaluated histologically, focal lesions were found in the livers of both groups, as foci, adenomas, and carcinomas. Moreover, the expression of AFP was confirmed to be upregulated at foci (Fig. 2b) and tumors (Fig. 2d) using immunohistochemistry for AFP, including in ABM*i* livers. The kinetics of tumor development were assessed by three factors: incidence, multiplicity, and size. At 4.5 months after DEN treatment, the incidence of foci in the livers of the ABM*i* group was significantly lower (control, 12/17 = 70.1%; ABM*i*, 4/23 = 17.4%; $P = 0.0004$) (Fig. 3a), and there was a smaller number (control, 2.01/cm^2; ABM*i*, 0.61/cm^2; $P = 0.003$) (Fig. 3b), while their size was almost equal (Ctrl, 0.51 mm^2; ABM*i*, 0.28 mm^2; $P = 0.35$) (Fig. 3c). In addition, there was a also a lower incidence of tumors (adenomas and carcinomas) in ABM*i* livers (control, 11/17 = 64.7%; ABM*i*, 7/23 = 30.4%; $P = 0.03$) (Fig. 3d) and a smaller number of tumors (control, 2.07/cm^2; ABM*i*, 0.62/cm^2; $P = 0.006$) (Fig. 3e), with no significant difference in their size (control, 4.70 mm^2; ABM*i*, 3.50 mm^2; $P = 0.43$) (Fig. 3f). These results confirmed that frequent ABM*i* might suppress tumor initiation in the DEN/GFP-CCl_4 model.

GFP-positive tumors were not found in ABM*i* livers

The repopulation of infused GFP-positive BMC in livers was examined by immunohistochemistry using GFP antibodies. It was confirmed that GFP-positive BMC were present, along with hepatic fibers, in surrounding liver, but not in focal lesions (Fig. 4). Moreover, no tumors composed of GFP-positive cells were observed.

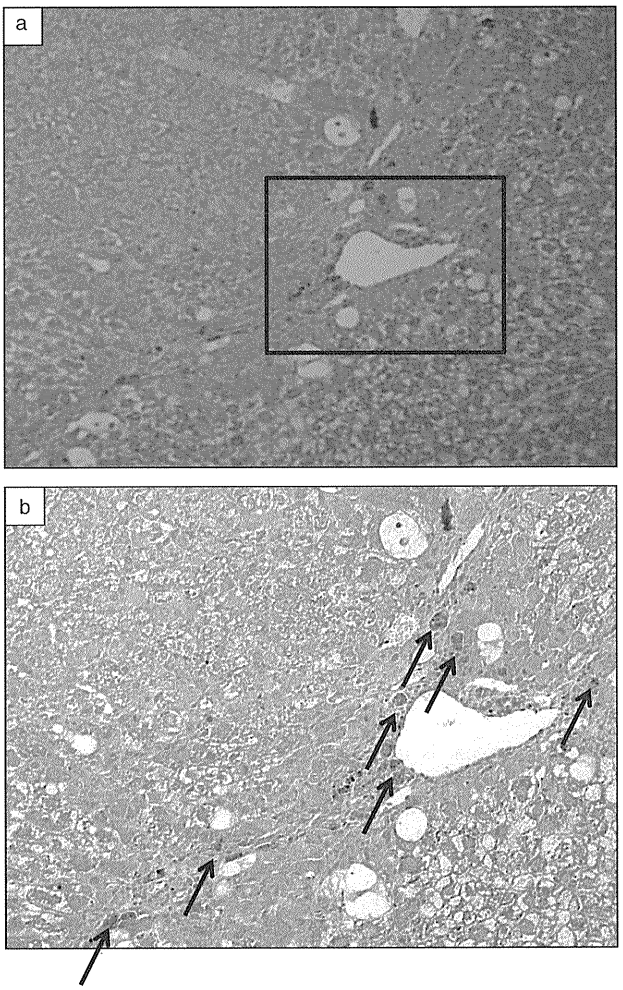

Figure 4 Repopulation of infused green fluorescent protein (GFP)-positive bone marrow cells in livers of the autologous bone marrow cell infusion group. (a,b) Immunohistochemical staining using anti-GFP antibodies. Original magnification is × 100 (a) and × 200 (b). Arrows in (b) show the GFP-positive cells in the surrounding liver of the GFP-positive bone marrow cell-infused mouse.

Liver fibrosis was reduced in ABM*i* livers

On Sirius red staining, liver fibrosis was significantly reduced after frequent ABM*i* ($P = 0.03$) (Fig. 5). This reduction in liver fibrosis was consistent with our previous observations in the GFP/CCl_4 model.[4]

Redox homeostasis was maintained in ABM*i* livers

Redox status was assessed in ABM*i* and control livers. Levels of 8-OHdG, one of the most abundant products of DNA oxidation, were significantly lower in ABM*i* livers ($P = 0.005$) (Fig. 6a). Concomitantly, hepatic SOD activity was also significantly higher in ABM*i* livers ($P = 0.01$) (Fig. 6b). SOD, which catalyzes the dismutation of the superoxide anion into hydrogen peroxide and